Carbohydrate Polymers 90 (2012) 1818–1825

Contents lists available at SciVerse ScienceDirect

Carbohydrate Polymers

journal homepage: www.elsevier.com/locate/carbpol

Synthesis of methylcellulose–silver nanocomposite and investigation of mechanical and antimicrobial properties

Dipanwita Maity[a], Md. Masud Rahaman Mollick[a], Dibyendu Mondal[a], Biplab Bhowmick[a], Mrinal Kanti Bain[a], Kalipada Bankura[a], Joy Sarkar[b], Krishnendu Acharya[b], Dipankar Chattopadhyay[a,*]

[a] Department of Polymer Science and Technology, University College of Science and Technology, University of Calcutta, 92 A.P.C. Road, Kolkata 700009, India
[b] Molecular and Applied Mycology and Plant Pathology Laboratory, Department of Botany, University of Calcutta, Kolkata 700019, India

ARTICLE INFO

Article history:
Received 1 June 2012
Received in revised form 30 July 2012
Accepted 31 July 2012
Available online 8 August 2012

Keywords:
Silver nanoparticles
Methylcellulose
Composite materials
Films
Mechanical property
Antimicrobial activity

ABSTRACT

In this paper we reported preparation of methylcellulose–silver nanocomposite films by mixing of aqueous solution of methylcellulose with silver nitrate followed by casting. The silver nanoparticles were generated in methylcellulose matrix through reduction and stabilization by methylcellulose. The surface plasmon band at 412 nm indicated the formation of Ag nanoparticles. The MC–Ag nanocomposite films were characterized by X-ray diffraction (XRD), transmission electron microscopy (TEM) and Fourier transform infrared (FTIR). The X-ray diffraction analysis of synthesized MC–Ag nanocomposite films revealed that metallic silver was present in face centered cubic crystal structure. Average crystallite size of silver nanocrystal was 22.7 nm. The FTIR peaks of as-synthesized MC–Ag nanocomposite fully designated the strong interaction between Ag nanoparticles and MC matrix. Nano-sized silver modified methylcellulose showed enhanced mechanical properties i.e. the introduction of Ag leading to both strengthening and toughening of MC matrix. The methylcellulose–silver nanocomposite films offered excellent antimicrobial activity against various microorganisms.

1. Introduction

Metal–polymer hybrid nanocomposites have recently attracted much attention owing to their potential to offer the synergistic features of polymeric materials with those of inorganic materials. Polymers are excellent host materials for nanoparticles of metal and semiconductor (Chandra et al., 2007; Liang, Bao, & Tjong, 2007; Mbhele et al., 2003; Mullick, Witcomb, & Scurrell, 2004; Singh & Khanna, 2007; Slistan-Grijalva et al., 2008; Wang, An, Luo, Li, & Li, 2008; Zhang & Han, 2003) along with different exceptional optical and electrical properties. Polymers behave as surface capping agents when the metal nanoparticles are embedded or encapsulated in them. The particle size is controlled well within the desired regime and the casting of films becomes easier from these metal–polymer hybrid systems (Yong et al., 2007; Zhao et al., 2007). Simultaneously, metal nanoparticles with high surface to bulk ratio drastically affect the polymer matrix leading to some unique properties unparallel to the pure materials. To predict the final properties of the nanocomposite, it is quite significant to investigate the influence of metal nanoparticles on the properties of a polymer matrix.

It is well known that the silver is superior to other metals in many fields. It has exceptionally good optical properties (Slistan-Grijalva et al., 2008; Stepanov, Popok, Khaibullin, & Kreibig, 2002), electrical conductivity (Chang & Yen, 1995), catalytic activity (Tarimala et al., 2006), surface enhanced Raman scattering (Setua et al., 2007) and antibacterial effects (Dubas, Kumlangdudsana, & Potiyaraj, 2006). One interesting aspect of nanotechnology concerns the formation of nanoparticles on a solid support such as a thin film, given potential for new devices involving photonics and plasmonics (Gradess et al., 2009). There have been a large number of reports on the fabrication of silver based nanocomposites (Cascaval et al., 2007; Leopold & Lendl, 2003; Manna, Batabyal, & Nandi, 2006; Schaaff & Rodinone, 2003). Two different approaches may be used to obtain metal–polymer nanocomposite films viz. ex situ and in situ method. In the ex situ approach, the metal nanoparticles synthesized through wet chemical routes is dispersed into a polymer solution which is finally spin coated to form a thin film (Akamatsu et al., 2000; Dirix, Bastiaansen, Caseri, & Smith, 1999; Khanna et al., 2005; Radheshkumar & Munstedt, 2005; Zeng et al., 2002; Zhang & Han, 2003). A high concentration of metal nanoparticles is sometimes required to get the desired properties of the final product. However, it is difficult to get homogeneous dispersion of high concentration of metal nanoparticles into the polymer matrix because of their ease of agglomeration at high concentration. In the latter metal nanoparticles are

* Corresponding author.
E-mail address: dipankar.chattopadhyay@gmail.com (D. Chattopadhyay).

0144-8617/$ – see front matter © 2012 Elsevier Ltd. All rights reserved.
http://dx.doi.org/10.1016/j.carbpol.2012.07.082

generated inside a polymer matrix by a chemical reduction of a metallic precursor present in the polymer thin film (Abargues et al., 2008; Compton et al., 2006; Dirix et al., 1999; Espuche et al., 2005; Gradess et al., 2009; Porel, Singh, Harsha, Rao, & Radhakrishnan, 2005; Thompson, Thompson, & Southward, 2002). This approach is more suitable for controlling the nanoparticle size and distribution in the polymer matrix and has the advantage of simplicity. Its processing simplicity and easy controlling of the nanoparticle size and distribution make this process widespread. Our previous work (Maity et al., 2011) is an example of such in situ approach.

Among the various inorganic metal nanoparticles, silver nanoparticles have received substantial attention for various reasons that the silver is an effective antimicrobial agent and exhibits low toxicity (Jain, Daima, Kachhwaha, & Kothari, 2009; Sondi & Salopek-Sondi, 2004). In small concentration, silver is safe for human cells, but lethal for bacteria and viruses (Saha et al., 2010; Sarkar, Saha, Chattopadhyay, Patra, & Acharya, 2011; Sharma, Yngard, & Lin, 2009). Reduction of the particle size of the material is an efficient and reliable tool for improving their biocompatibility that can be achieved using nanotechnology.

Cellulose, the most abundant biomass and renewable resource on earth, is biodegradable, biocompatible and non toxic in nature. It can be converted into cellulose derivative and regenerated materials (Klemm, Heublein, Fink, & Bohn, 2005). More recently cellulose based nanocomposite and their derivatives have attracted great attention and showed more and more importance due to their high value-added application in science and technology (Deng, Zhou, Du, Van Kasteren, & Wang, 2009; Liu, Zhang, Zhou, & Wu, 2008; Ruan, Huang, & Zhang, 2005). However, there have been only few reports on the fabrication of bacterial cellulose–silver nanocomposite (Li, Jia, Ma, et al., 2011; Li, Jia, Zhu, et al., 2011). For example, the synthesis of bacterial cellulose silver nanocomposite with strong antimicrobial activity by immersing bacterial cellulose in silver nitrate solution using sodium borohydride as reducing agent is reported (Maneerung, Tokura, & Rujiravanit, 2008). Maria et al. synthesized bacterial cellulose/silver nanocomposites using different reductants (hydrazine, hydroxylamine or ascorbic acid) together with gelatin or polyvinylpyrrolidone (Maria et al., 2009). The synthesis of bacterial cellulose–silver nanocomposites and their performances as surface enhanced Raman scattering substrates has been studied and reported (Marques, Nogueira, Pinto, Neto, & Trindade, 2008). Zhu, Xue, and He (2009) detailed in situ synthesis of silver nanoparticles in natural cellulose fibers using sodium borohydride as reductant. The synthesis of silver nanoparticles by microwave heating method using sodium carboxymethylcellulose (CMC) as a stabilizing agent is stated in 2008 (Chen, Wang, Zhang, & Jin, 2008). Bhui et al. (2011) also studied the formation of silver nano structure of variable morphologies formed by methylcellulose (MC) at different temperature. But nevertheless no detailed study of MC–Ag nanocomposite films has been reported in the literature.

Here, we detail a simple one step in situ synthesis of methylcellulose–silver nanocomposite using silver nitrate, sodium hydroxide and methylcellulose solution. The synthesized MC–Ag nanocomposite is quite inexpensive and nontoxic. From the industrial viewpoint, this environmentally benign technique using aqueous media of biocompatible polysaccharide under ambient condition may be figured for the mass production of MC–Ag nanocomposites. Herein, we have studied the influence of the silver content on the mechanical properties of nanocomposite films in accordance with the optical and morphological analysis at different pH. Furthermore, the cup plate method is employed to evaluate their antimicrobial efficacy of these nanocomposites against different bacterial species.

2. Experimental

2.1. Materials

A cellulose derivative, methylcellulose (29.6% methoxyl content, viscosity 4000 cps) with the trade name Metolose SM 4000 (MC) was obtained from Shinetsu Chemical Co. Ltd., Japan. Silver nitrate ($AgNO_3$) and sodium hydroxide (NaOH) were purchased from Merck, India. All the chemicals were analytical grade reagent and were used as received without further purification.

2.2. Synthesis of methylcellulose–silver nanocomposites

The MC solution (1 wt%) was prepared by dispersing the required amount in distilled water with continuous stirring until completely dissolved. Then the solution was kept in refrigerator for 48 h to get a transparent MC solution (Neely, 1963).

A freshly prepared cold aqueous $AgNO_3$ (10^{-2} M) solution was added drop by drop to 90 ml aqueous methylcellulose solution in a conical flask to performs the Ag^+ to Ag^0 reaction in templates of methylcellulose molecules. Three sets of the above reaction mixture were taken in three different conical flasks. The pH of the solution was maintained using a small amount of NaOH (1 M) solution. The containers were wrapped by black paper and kept in dark to avoid any early $AgNO_3$ photo reduction. The solution turned pale yellow, golden yellow and reddish yellow with increasing pH. After 24 h the UV–vis spectra was recorded. The viscous MC–Ag samples obtained after 24 h were cast in the form of nanocomposite films, which was summarized in Fig. 1. Finally, after evaporation of the solvent, yellow transparent MC–Ag nanocomposite films were obtained. The films were dried at room temperature in air for 72 h. Their average thickness was about 0.03 ± 0.005 mm. Pure methylcellulose (MC) film sample was prepared in the same manner.

2.3. Characterization

The nanoparticles formation was monitored by the UV–vis spectra using a UV–vis spectrophotometer system (Agilent 8453 Spectrophotometer, USA). UV–vis study was done using a quartz cell of thickness of 1 cm in the wavelength range 190–1100 nm. X-ray diffraction measurements of methylcellulose (MC) and MC–Ag nanocomposite films were performed at room temperature by X-PERT-PRO Panalytical diffractometer at an accelerating voltage of 40 kV using Cu Kα ($\lambda = 1.5406$ Å) as X-ray source. FTIR spectrophotometer (Shimadzu FTIR-8400S) was used to identify the ingredients of the nanocomposite films. The thickness of the films was prepared in the range of 0.03 ± 0.005 mm. The shape, size and dispersity of the silver nanoparticles were monitored by transmission electron microscopy (HRTEM, model JEM 2010 EM) at an accelerating voltage of 200 kV and fitted with a CCD camera. A specimen for TEM study was made by casting a drop of sample suspension on a carbon coated copper grid allowed to air dry. The tensile strength, elongation at break and tensile modulus values of virgin MC and MC–Ag nanocomposite films were investigated using a universal testing machine (Zwick Roell) with a cross head speed of 5.0 mm/min for a gauge length of 50 mm and 14 mm in width at ambient temperature. The reported values were taken from an average of five measurements.

2.4. Assay for antimicrobial activity of silver nanoparticles against microorganisms

The silver nanoparticles in sterilized distilled water were tested for their antibacterial activity by the agar diffusion method. Five bacterial strains, *Bacillus subtilis* [MTCC 736], *Bacillus cereus* [MTCC 306], *Pseudomonas aeruginosa* [MTCC 8158], *Staphylococcus aureus*

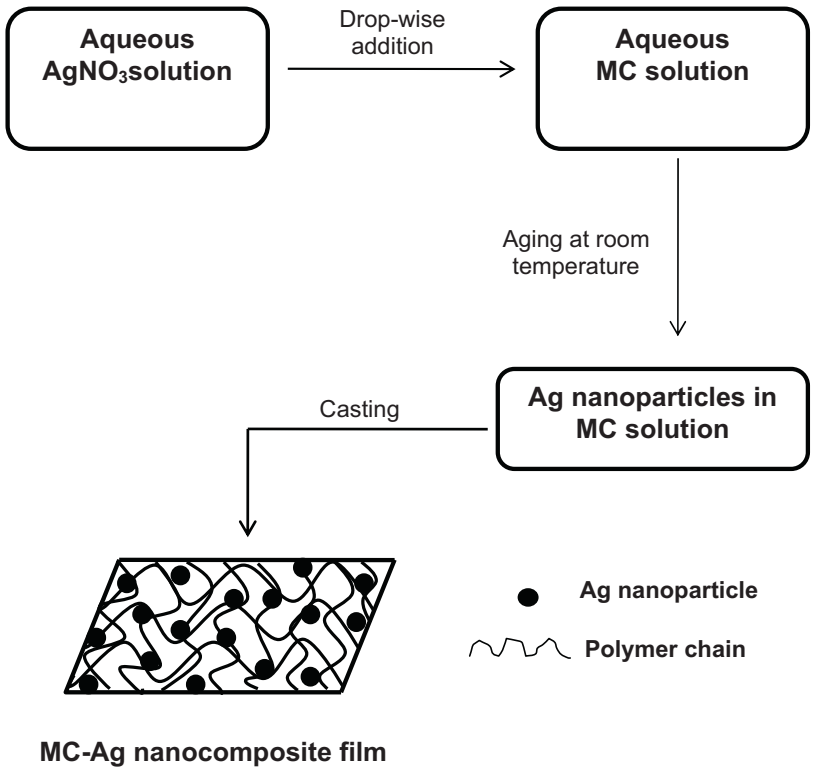

Fig. 1. Schematic representation of MC–Ag nanocomposite film preparation process.

[MTCC 96] and *Escherichia coli* [MTCC 68] along with the silver nitrate solution (10^{-3} M) as a control set were used for this analysis. These bacteria were grown on liquid nutrient agar media (HiMedia Laboratories Pvt. Ltd., Mumbai, India) for 24 h prior to the experiment, were seeded in agar plates by the pour plate technique. For every bacterial strain, four different cavities were made in one petri plate using a cork borer (10 mm diameter) at more or less equal distance. The cavities were filled with silver nitrate solution (10^{-3} M), 1 wt% methylcellulose, silver nanoparticles solution (0.2 mg/ml) and only sterile distilled water respectively. All the different plates containing the different bacterial strain were incubated at 37 °C for 24 h. Every experiment was repeated for three times.

3. Results and discussion

3.1. Optical and FTIR spectroscopy of the methylcellulose–silver nanocomposites

The UV–vis spectral analysis is carried out with the objective to establish the presence of silver nanoparticles in MC solution. Fig. 2 shows the absorption spectra of silver colloids in MC solution at different pH. The spectrum shows maximum absorbance at 412 nm. This well-defined sharp peak occurs due to the surface plasmon resonance band of silver colloids (Carotenuto, 2001). The peak ensures the formation of spherical silver nanoparticles similar to the synthesis of silver nanoparticles in aqueous Ag–PVA solution (Gautam & Ram, 2010). The data also resembles to the fabrication of PVP films with silver nanoparticles by ultra sound in ethylene glycol by G. Carotenuto. It is quite clear from Fig. 2 that the absorption intensity increases with increasing pH of the parent solution suggesting that the increase in pH facilitates the formation silver (Ag^0) from silver nitrate. At comparatively higher pH, NaOH facilitates the release of electrons from methylcellulose molecule to reduce the silver ions to form silver atoms. The maximum intensity of the plasmon peak at high pH indicates complete reduction of the silver ions (Raveendran, Fu, & Wallen, 2003) and therefore, reflecting the dual role of MC as stabilizing as well as reducing agent. Earlier report accounted that the position of the surface plasmon absorption peak of spherical colloidal silver particles depends on the refractive index of the surrounding medium, particle size and adsorbed substances on their surfaces. Mulvaney (1996) proposed that the position of the surface plasmon band of spherical colloidal silver particles in aqueous solution showed the absorption band at 382 ± 1 nm whereas a red shift at 433 nm is observed with Ag–PVA solution clearly demonstrating the effect of refractive index of PVA. This experimental result agrees with theoretical predictions, which indicate that the position of the surface plasmon absorption band of

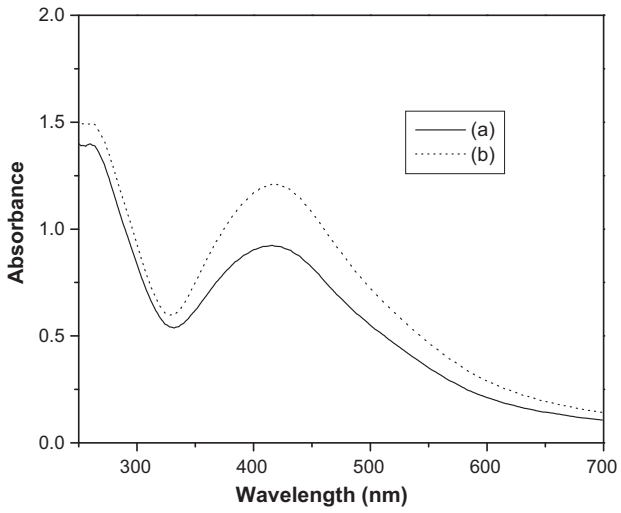

Fig. 2. UV–vis absorption spectra of methylcellulose–silver nanocomposite prepared at (a) pH 7, (b) pH10.

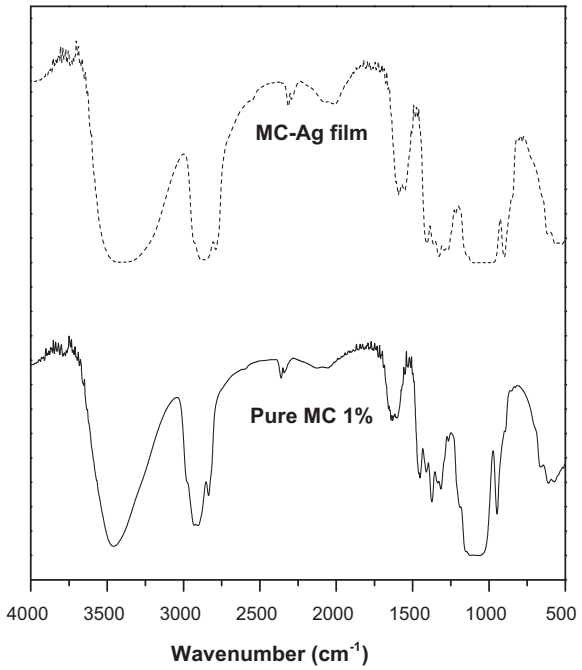

Fig. 3. FTIR spectra of MC and MC–Ag nanocomposite film.

silver particles embedded in solid polymer matrix shifts to longer wavelengths (Slistan-Grijalva et al., 2005) (Figs. 3 and 4).

The MC–Ag nanocomposites are further examined by FTIR analysis, as shown in Fig. 3. All the samples have almost similar peaks and exhibit the characteristics peaks of MC. For the MC molecule the band central at 3469 cm^{-1} can be attributed to the stretching vibration of hydroxyl group whereas the band at 2921 cm^{-1} is assigned to the asymmetric stretching vibration of C—H in pyranoid ring. 1641 cm^{-1} corresponds to the C—H bending mode; the absorption band at 1081 cm^{-1} is ascribed to C—O—C stretching mode from glucosidic units (Suflet, Chitanu, & Popa, 2006). The peak at 951 cm^{-1} is related to OCH_3 group. In the MC–Ag nanocomposite, the absorption band related to O—H stretching is at 3459 cm^{-1}, C—H stretching and bending at 2878 cm^{-1} and 1597 cm^{-1} respectively. The peak at 1051 cm^{-1} and 908 cm^{-1} is due to C—O—C stretching mode from the glucosidic unit and the OCH_3 group of MC respectively. It is important to note that the broad peak at around 3459 cm^{-1} become broader in MC–Ag nanocomposite compare with pure MC. For all the MC–Ag films have been desiccated in vacuum to remove water before carrying out the FTIR measurement. A similar phenomenon in cellulose-based nanocomposites is reported for cellulose–Fe_2O_3 nanocomposites (Liu et al., 2008). All absorption bands in nanocomposite films are shifted and also the band 1081 cm^{-1} became broader, further indicating a strong interaction between Ag nanoparticles and MC matrix.

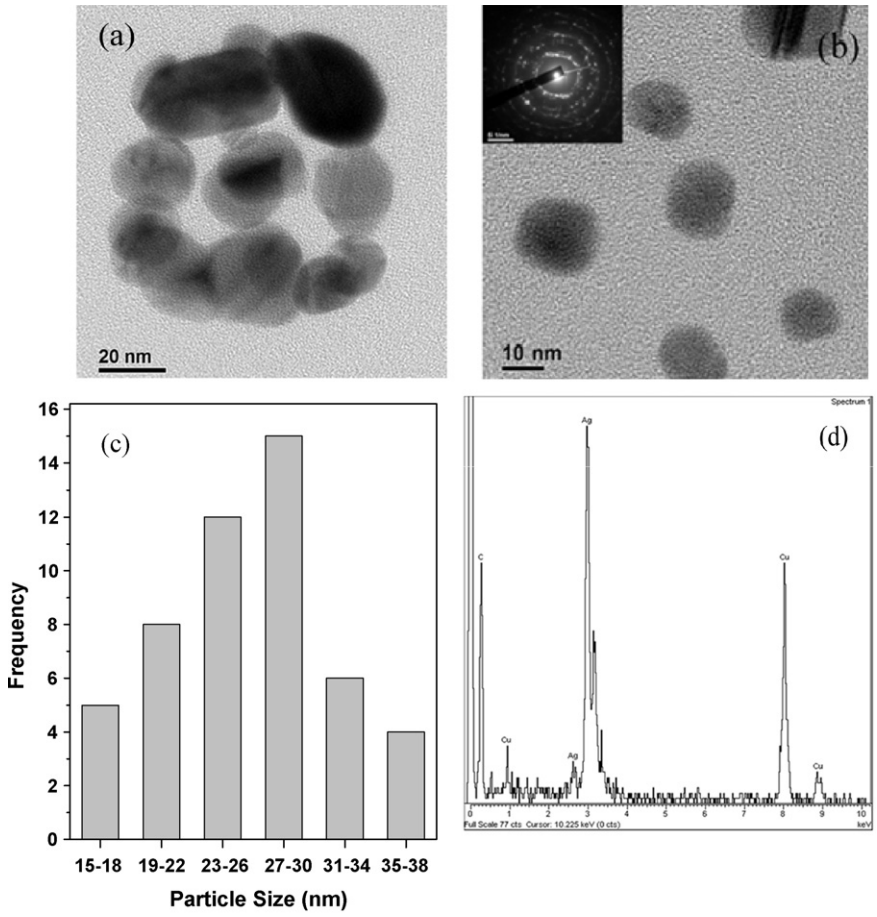

Fig. 4. (a) HRTEM image of silver nanoparticles prepared at pH 7 using 10^{-2} M aqueous solution of $AgNO_3$ in 1 wt% MC at ambient temperature. (b) HRTEM image of silver nanoparticles prepared at pH 10 using 10^{-2} M aqueous solution of $AgNO_3$ in 1 wt% MC at ambient temperature. Inset shows the selected area electron diffraction (SAED) image. (c) Particle size distribution histogram of silver nanoparticles determined from HRTEM micrograph prepared at pH 10. (d) Energy dispersive X-ray of silver nanoparticles.

3.2. Morphology and structure of the methylcellulose–silver nanocomposites

To get the confirmation of the formation of silver nanoparticles and a deep insight in the morphology of the silver nanoparticles, high-resolution transmission electron microscopic analysis is performed. Fig. 4(a) represents the TEM micrograph of MC–Ag nanocomposite in presence of 1% of MC and 10^{-2} M of $AgNO_3$ prepared at pH 7. From the Fig. 4(a), it is clear that the particles are not well dispersed and there is a tendency to form agglomerates. On the other hand, at pH 10 in Fig. 4(b) particles are spherical, well dispersed with uniform size distribution. No agglomeration is observed at higher pH. It is clear from Fig. 4(c) that the silver nanoparticles are of 10–40 nm and posses an average size of 22 nm. In addition, the selected area electron diffraction (SAED) patterns of MC–Ag nanocomposite in the inset of Fig. 4(b) shows the crystalline character and ordered orientations of the lattice fringe of the silver nanoparticles. This is in agreement with the X-ray diffraction result, i.e. the SAED pattern showing rings with diffraction points ascribed to (1 1 1), (2 0 0), (2 2 0) and (3 1 1) confirm the face centered cubic (fcc) crystalline structure of silver. There are some sharp spots distributed in the diffraction patterns, which are due to larger silver nanoparticles. The energy dispersive X-ray spectroscopy (EDX) in Fig. 4(d) proves the formation of silver nanoparticles. The EDX spectrum is taken from a random assembly of Ag nanoparticles. The signal of Cu is originated from the carbon coated Cu grid. TEM result demonstrates the formation of MC–Ag nanocomposite films.

The XRD diffraction studies of MC and MC–Ag nanocomposite films are carried out to establish the presence of nanosilver in MC films and also to determine crystal structure of silver and to calculate particle size using Scherrer equation. The XRD pattern of virgin methylcellulose and as prepared MC–Ag nanocomposite films is represented in Fig. 5. The diffraction peak at around $2\theta = 8.13^\circ$ and 20.63° correspond to the typical diffraction pattern of methylcellulose (Li, Jia, Ma, et al., 2011; Li, Jia, Zhu, et al., 2011). The peak at 8.13° is a clear evidence of cellulose modification. This peak position indicates an increase in inter-planner distance in relation to the original cellulose. This occurs due to the generation of disorder during modification. The projection of substituting groups along the axis (—CH3 groups) is associated with an increase in interfibrillar distance. The peak at 20.63° confirms the crystallinity present in the methylcellulose molecule due to the strong intermolecular and intramolecular hydrogen bonding between the methylcellulose molecular chains. The diffraction

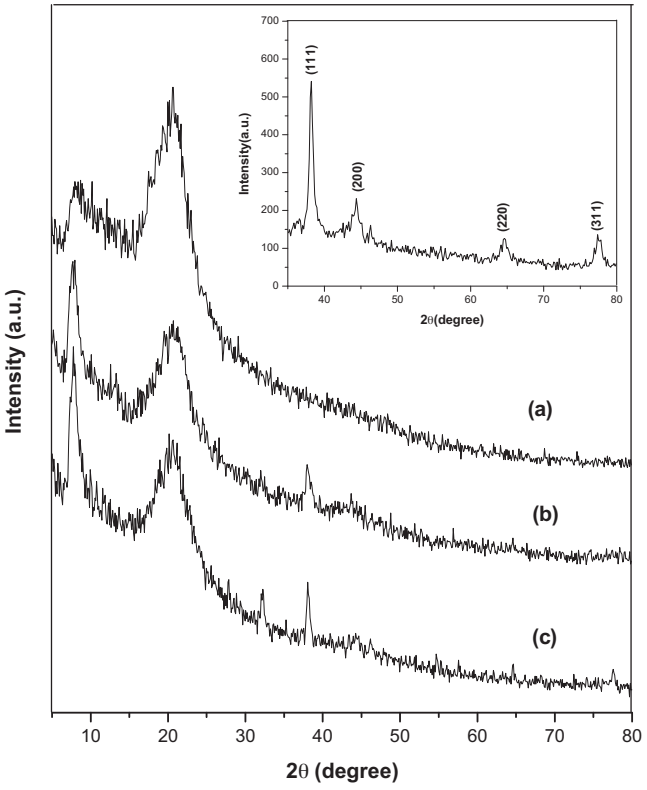

Fig. 5. X-ray diffraction of (a) virgin MC, (b) MC–Ag nanocomposite film prepared at pH 7, (c) MC–Ag nanocomposite film prepared at pH 10. Inset shows the XRD pattern of MC–Ag nanocomposite.

peaks at $(2\theta) = 38.1^\circ$, 44.2°, 64.6° and 77.3° are assigned as (1 1 1), (2 0 0), (2 2 0) and (3 1 1) planes of well crystallized silver with a cubic structure (JCPDS 04-0783), suggesting the successful synthesis of silver using methylcellulose which is clearly shown in Fig. 5. Applying the Scherrer equation with the Ag (1 1 1) peak data the average crystallite size is ~22.7 nm. Comparatively low diffraction intensity of Ag in the MC–Ag nanocomposite film may be due to the low concentration of Ag than methylcellulose. The result is quite evident in response of the formation of MC–Ag nanocomposite films.

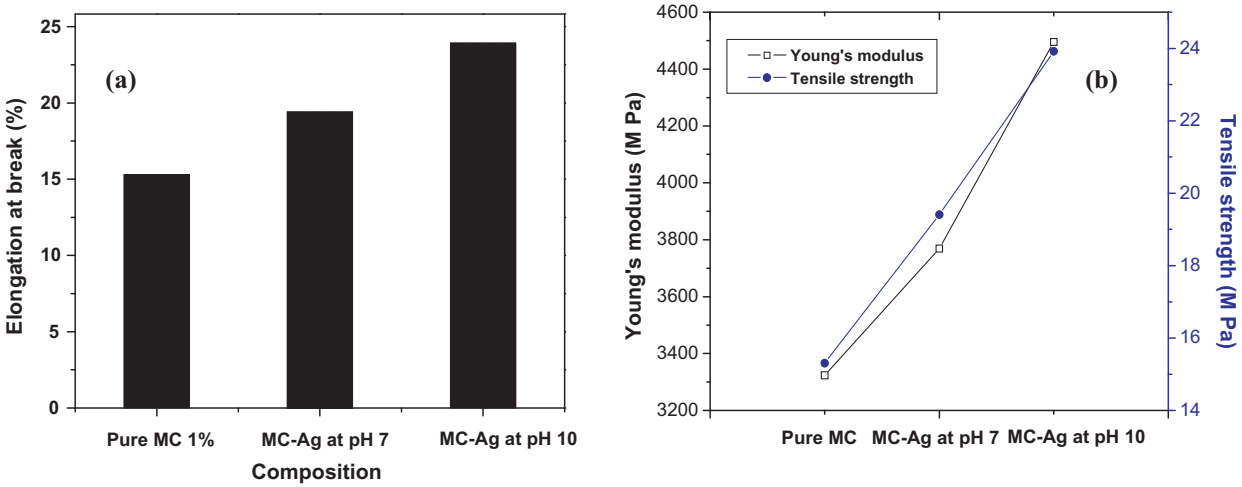

Fig. 6. (a) Elongation at break, (b) Young's modulus and tensile strength of MC and MC–Ag nanocomposite films prepared at different pH.

3.3. Mechanical properties of the methylcellulose–silver nanocomposites

The mechanical properties such as elongation at break (%), tensile strength and Young's modulus of the MC–Ag nanocomposite films at different pH are measured and compared with the virgin MC film. Fig. 6(a) shows the elongation at break (%) of pure MC and MC–Ag nanocomposite films prepared at pH 7 and pH 10. It is clear from Fig. 6(a) that the elongation at break (%) of pure MC increases from 15.31 to 19.41 and 23.92 in case of MC–Ag nanocomposites prepared at pH 7 and pH 10 respectively. Fig. 6(b) shows tensile properties of pure MC and its nanocomposite films vs pH. Tensile tests are performed on the sample in a relative humidity of 50%. From the Fig. 6(b), it is clear that the tensile strength of MC–Ag nanocomposite films increases with increasing pH up to 10. The tensile strength of pure MC film is 58.14 Mpa and increases to 66.95 Mpa and 78.71 Mpa in case of MC–Ag nanocomposites synthesized at pH 7 and pH 10 respectively. So, it can be concluded that the tensile strength of MC–Ag nanocomposite films prepared at pH 7 and pH 10 increases by 15.16% and 35.38% respectively compared to pure MC film. This indicates the strong interactions between MC molecules and Ag nanoparticles. The Young's modulus of the MC–Ag film increases linearly with increasing pH of the solution. From the Fig. 6(b), it is also observed that the tensile modulus at 1% strain is found to increase from 3232.80 MPa for pure MC to 3769.04 MPa and 4495.01 MPa for MC–Ag nanocomposite films prepared at pH 7 and 10 respectively. Therefore the tensile modulus is increased by 13.39% and 35.24% compared to that of pure MC.

Thus from the above observation at a certain pH range, it can be concluded that the introduction of Ag will lead to both strengthening and toughening of the MC matrix. The nanoparticles affect the structural rearrangements during the post-elastic deformation to induce semi crystalline like mechanical behavior. This type of feature sometimes observed in case of polymer–metal nanocomposites (Mbhele et al., 2003).

3.4. Antimicrobial activity of the silver nanoparticles against microorganisms

The silver nanoparticle solution exhibited excellent antibacterial activity against the bacteria, *B. subtilis*, *B. cereus*, *P. aeruginosa*, *S. aureus* and *E. coli* by showing the clearing zones around the holes with bacterial growth on petri plates by cup plate method. The radial diameter of the inhibiting zones of *B. subtilis*, *B. cereus*, *E. coli*, *S. aureus* and *P. aeruginosa* are 28, 24, 20, 18, 17 mm respectively. Silver nanoparticles at the concentration of 0.2 mg/ml showed a range of specificity towards its antimicrobial activity (Fig. 7). Fig. 8 represented the clear inhibition zones made by silver nitrate solution (a) and silver nano particle solution (c) respectively against the strain of *B. subtilis* only. The clear zone indicated bacterial growth restriction by diffused silver nanoparticles as well as silver nitrate solution. At the same time methylcellulose solution (b) and sterile distilled water (d) did not show any inhibition zone in the same figure. Results are mean of three separate experiments, each in triplicate. It is reported in literature that several silver containing salts showed a good antimicrobial activity (Rai, Yadav, & Gade, 2009). But the higher concentration of silver was harmful to both consumer and the microbes. That is why the smaller concentration (nano range) is much more applicable for that purpose. These results clearly indicate that the anti bacterial activity is only due to the silver nanoparticles and not due to the methylcellulose.

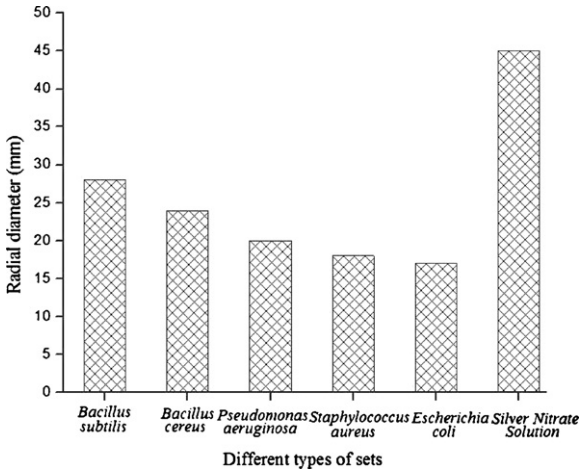

Fig. 7. Radial diameter of inhibitory zone by Ag nanoparticles (0.2 mg/ml) against different microorganisms.

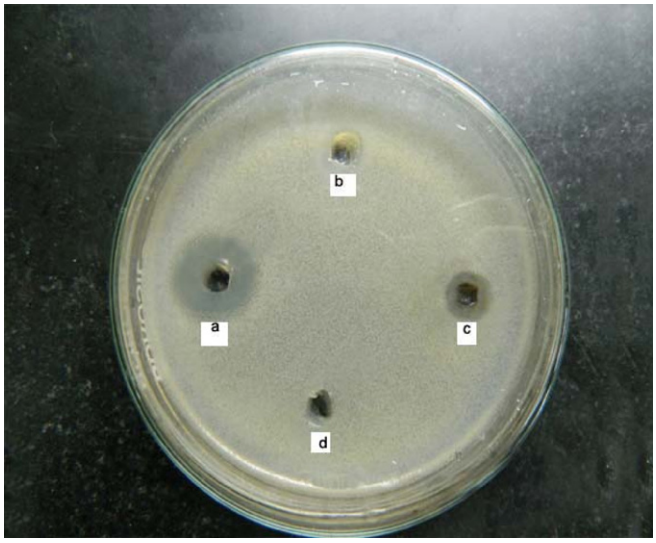

Fig. 8. Antimicrobial activity of (a) silver nitrate solution, (b) methylcellulose solution, (c) silver nanoparticle solution and (d) sterile distilled water against the strain of *Bacillus subtilis*.

4. Conclusion

In summary, we have described a simple, rapid synthesis route to prepare methylcellulose–silver nanocomposite films. This process does not need any seed, template or surfactant, thus is a convenient and fast pathway for large-scale and low cost production of silver modified methylcellulose nanocomposite films. UV–vis absorption spectra shows characteristic peak of the surface plasmon resonance of silver nanoparticles. XRD and FT-IR results implied that the obtained samples are methylcellulose–silver nanocomposite films. TEM analysis confirmed the presence of Ag nanoparticles of average size ~22 nm in MC–Ag nanocomposite films. Nano-sized silver modified methylcellulose shows enhanced mechanical properties like tensile strength, young modulus etc. and the introduction of Ag leads to both strengthening and toughening of MC matrix. Similarly, other metallic nanoparticles–polymer nanocomposites could also be synthesized from appropriate metal salt precursors. The methylcellulose–silver nanocomposites exhibit a strong antibacterial activity against microorganisms. Moreover, the methylcellulose–silver nanocomposites films described here are expected to have good potential performance as functional

materials in future, which can also open a new application for methylcellulose.

Acknowledgments

The authors D. Maity gratefully acknowledge UGC, Govt. of India for her fellowship, M.M.R.M likes to thank DST for his fellowship under INSPIRE fellowship and D. Mondal thank CSIR, New Delhi for his fellowship.

References

Abargues, R., Marqués-Hueso, J., Canet-Ferrer, J., Pedrueza, E., Valdés, J. L., Jiménez, E., et al. (2008). High-resolution electron-beam patternable nanocomposite containing metal nanoparticles for plasmonics. *Nanotechnology*, *19*, 355308–355314.

Akamatsu, K., Takei, S., Mizuhata, M., Kajinami, A., Deki, S., Takeoka, S., et al. (2000). Preparation and characterization of polymer thin films containing silver and silver sulfide nanoparticles. *Thin Solid Films*, *359*, 55–60.

Bhui, D. K., Pyne, S., Sarkar, P., Bar, H., Sahoo, G. P., & Misra, A. (2011). Temperature controlled synthesis of silver nanostructures of variable morphologies in aqueous methyl cellulose matrix. *Journal of Molecular Liquid*, *158*, 170–174.

Carotenuto, G. (2001). Synthesis and characterization of poly(*N*-vinylpyrrollidone) filled by monodispersed silver cluster with controlled size. *Applied Organometallic Chemistry*, *15*, 344–351.

Cascaval, C. N., Cristea, M., Rosu, D., Ciobanu, C., Paduraru, O., & Cotofana, C. (2007). Preparation and characterization of polyvinyl alcohol–colloidal silver nanocomposites. *Journal of Optoelectronics and Advanced Materials*, *9*, 2116–2120.

Chandra, A., Turng, L. S., Gong, S. Q., Hall, D. C., Caulfield, D. F., & Yang, H. (2007). Study of polystyrene/titanium dioxide nanocomposites via melt compounding for optical applications. *Polymer Composite*, *28*, 241–250.

Chang, L. T., & Yen, C. C. (1995). Studies on the preparation and properties of conductive polymers: Use of heat-treatment to prepare metallized films from silver chelate of PVA and PAN. *Journal of Applied Polymer Science*, *55*, 371–374.

Chen, J., Wang, J., Zhang, X., & Jin, Y. L. (2008). Microwave-assisted green synthesis of silver nanoparticles by carboxymethyl cellulose sodium and silver nitrate. *Material Chemistry and Physics*, *108*, 421–424.

Compton, J., Thompson, D., Kranbuehl, D., Ohl, S., Gain, O., David, L., et al. (2006). Hybrid films of polyimide containing in situ generated silver or palladium nanoparticles: Effect of the particle precursor and of the processing conditions on the morphology and the gas permeability. *Polymer*, *47*, 5303–5313.

Deng, M. L., Zhou, Q., Du, A. K., Van Kasteren, J., & Wang, Y. Z. (2009). Preparation of nanoporous cellulose foams from cellulose-ionic liquid solutions. *Material Letter*, *63*, 1851–1854.

Dirix, Y., Bastiaansen, C., Caseri, W., & Smith, P. (1999). Preparation, structure and properties of uniaxially oriented polyethylene–silver nanocomposites. *Journal of Material Science*, *34*, 3859–3866.

Dubas, S. T., Kumlangdudsana, P., & Potiyaraj, P. (2006). Layer-by-layer deposition of antimicrobial silver nanoparticles on textile fibers. *Colloids and Surfaces A: Physicochemical and Engineering Aspects*, *289*, 105–109.

Espuche, E., David, L., Rochas, C., Afeld, J. L., Compton, J. M., Thompson, D. W., et al. (2005). In situ generation of nanoparticulate lanthanum(III) oxide-polyimide films: Characterization of nanoparticle formation and resulting polymer properties. *Polymer*, *46*, 6657–6665.

Gautam, A., & Ram, S. (2010). Preparation and thermomechanical properties of Ag-PVA nanocomposite films. *Material Chemistry and Physics*, *119*, 266–271.

Gradess, R., Abargues, R., Habbou, A., Canet-Ferrer, J., Pedrueza, E., Russell, A., et al. (2009). Localized surface plasmon resonance sensor based on Ag-PVA nanocomposite thin films. *Journal of Material Chemistry*, *19*, 9233–9240.

Jain, D., Daima, H. K., Kachhwaha, S., & Kothari, S. L. (2009). Synthesis of plant-mediated silver nanoparticles using papaya fruit extract and evaluation of their anti microbial activities. *Digest Journal of Nanomaterials and Biostructures*, *4*, 557–563.

Khanna, P. K., Singh, N., Charan, S., Subbarao, V. V. V. S., Gokhale, R., & Mulik, U. P. (2005). Synthesis and characterization of Ag/PVA nanocomposite by chemical reduction method. *Materials Chemistry and Physics*, *93*, 117–121.

Klemm, D., Heublein, B., Fink, H. P., & Bohn, A. (2005). Cellulose: Fascinating biopolymer and sustainable raw material. *Angewandte Chemie International Edition*, *44*, 3358–3393.

Leopold, N., & Lendl, B. (2003). A new method for fast preparation of highly surface enhanced Raman scattering (SERS) active silver colloids at room temperature by reduction of silver nitrate with hydroxylamine hydrochloride. *Journal of Physical Chemistry B*, *107*, 5723–5727.

Li, S.-M., Jia, N., Ma, M.-G., Zhang, Z., Liu, Q.-H., & Sun, R.-C. (2011). Cellulose–silver nanocomposites: Microwave-assisted synthesis, characterization, their thermal stability and antimicrobial property. *Carbohydrate Polymers*, *86*, 441–447.

Li, S.-M., Jia, N., Zhu, J.-F., Ma, M.-G., Xu, F., Wang, B., et al. (2011). Rapid microwave-assisted preparation and characterization of cellulose–silver nanocomposites. *Carbohydrate Polymers*, *83*, 422–429.

Liang, G. D., Bao, S. P., & Tjong, S. C. (2007). Microstructure and properties of polypropylene composites filled with silver and carbon nanotube nanoparticles prepared by melt-compounding. *Materials Science and Engineering B*, *142*, 55–61.

Liu, S. L., Zhang, L. N., Zhou, J. P., & Wu, R. X. (2008). Structure and properties of cellulose/Fe_2O_3 nanocomposite fibers spun via an effective pathway. *Journal of Physical Chemistry C*, *112*, 4538–4544.

Maity, D., Bain, M. K., Bhowmick, B., Sarkar, J., Saha, S., Acharya, K., et al. (2011). In situ synthesis, characterization, and antimicrobial activity of silver nanoparticles using water soluble polymer. *Journal of Applied Polymer Science*, *122*, 2189–2196.

Maneerung, T., Tokura, S., & Rujiravanit, R. (2008). Impregnation of silver nanoparticles into bacterial cellulose for antimicrobial wound dressing. *Carbohydrate Polymers*, *72*, 43–51.

Manna, S., Batabyal, S. K., & Nandi, A. K. (2006). Preparation and characterization of silver–poly(vinylidene fluoride) nanocomposites: Formation of piezoelectric polymorph of poly(vinylidene fluoride). *Journal of Physical Chemistry B*, *110*, 12318–12326.

Maria, L. C. D., Santos, A. L. C., Oliveira, P. C., Barud, H. S., Messaddeq, Y., & Ribeiro, S. J. L. (2009). Synthesis and characterization of silver nanoparticles impregnated into bacterial cellulose. *Material Letters*, *63*, 797–799.

Marques, P. A. A. P., Nogueira, H. I. S., Pinto, R. J. B., Neto, C. P., & Trindade, T. (2008). Silver-bacterial cellulosic sponges as active SERS substrates. *Journal of Raman Spectroscopy*, *39*, 439–443.

Mbhele, Z. H., Salemane, M. G., van Sittert, C. G. C. E., Nedeljkovic, J. M., Djokovic, V., & Luyt, A. S. (2003). Fabrication and characterization of silver–polyvinyl alcohol nanocomposites. *Chemistry of Materials*, *15*, 5019–5024.

Mullick, K., Witcomb, M. J., & Scurrell, M. S. (2004). Polymer stabilized silver nanoparticles: A photochemical synthesis route. *Journal of Material Science*, *39*, 4459–4463.

Mulvaney, P. (1996). Surface plasmon spectroscopy of nanosized metal particles. *Langmuir*, *12*, 788–800.

Neely, W. B. (1963). Solution properties of polysaccharides. IV. Molecular weight and aggregate formation in methylcellulose solutions. *Journal of Polymer Science Part A: General Papers*, *1*, 311–320.

Porel, S., Singh, S., Harsha, S. S., Rao, D. N., & Radhakrishnan, T. P. (2005). Nanoparticle-embedded polymer: In situ synthesis, free-standing films with highly monodisperse silver nanoparticles and optical limiting. *Chemistry of Materials*, *17*, 9–12.

Radheshkumar, C., & Munstedt, H. (2005). Morphology and mechanical properties of antimicrobial polyamide/silver composites. *Material Letters*, *59*, 1949–1953.

Rai, M., Yadav, A., & Gade, A. (2009). Silver nanoparticles as a new generation of antimicrobials. *Biotechnology Advances*, *27*, 76–83.

Raveendran, P., Fu, J., & Wallen, S. L. (2003). Completely "green" synthesis and stabilization of metal nanoparticles. *Journal of the American Chemical Society*, *125*, 13940–13941.

Ruan, D., Huang, Q. L., & Zhang, L. N. (2005). Structure and properties of CdS/regenerated cellulose nanocomposites. *Macromolecular Materials and Engineering*, *290*, 017–1024.

Saha, S., Sarkar, J., Chattopadhyay, D., Patra, S., Chakraborty, A., & Acharya, K. (2010). Production of silver nanoparticles by a phytopathogenic fungus *Bipolaris nodulosa* and its antimicrobial activity. *Digest Journal of Nanomaterials and Biostructures*, *5*, 887–895.

Sarkar, J., Saha, S., Chattopadhyay, D., Patra, S., & Acharya, K. (2011). Mycosynthesis of silver nanoparticles and investigation of their antimicrobial activity. *Journal of Nanoscience, Nanoengineering and Applications*, *1*, 17–26.

Schaaff, T. G., & Rodinone, A. J. (2003). Preparation and characterization of silver sulfide nanocrystals generated from silver (I)-thiolate polymers. *Journal of Physical Chemistry B*, *107*, 10416–10422.

Setua, P., Chakraborty, A., Seth, D., Bhatta, M. U., Satyam, P. V., & Sarkar, N. (2007). Synthesis, optical properties and surface enhanced Raman scattering of silver nanoparticles in nonaqueous methanol reverse micelles. *Journal of Physical Chemistry C*, *111*, 3901–3907.

Sharma, V. K., Yngard, R. A., & Lin, Y. (2009). Silver nanoparticles: Green synthesis and their microbial activities. *Advances in Colloid and Interface Science*, *145*, 83–96.

Singh, N., & Khanna, P. K. (2007). In situ synthesis of silver nano-particles in polymethylmethacrylate. *Material Chemistry and Physics*, *104*, 367–372.

Slistan-Grijalva, A., Herrera-Urbina, R., Rivas-Silva, J. F., Avalos Borja, M., Castillon-Barraza, F. F., & Posada-Amarillas, A. (2005). Classical theoretical characterization of the surface plasmon absorption band for silver spherical nanoparticles suspended in water and ethylene glycol. *Physica E*, *27*, 104–112.

Slistan-Grijalva, A., Herrera-Urbina, R., Rivas-Silva, J. F., Ávalos-Borja, M., Castillón-Barraza, F. F., & Posada-Amarillas, A. (2008). Synthesis of silver nanoparticles in a polyvinylpyrrolidone (PVP) paste, and their optical properties in a film and in ethylene glycol. *Materials Research Bulletin*, *43*, 90–96.

Sondi, I., & Salopek-Sondi, B. (2004). Silver nanoparticles as antimicrobial agent: a case study on *E. coli* as a model for Gram-negative bacteria. *Journal of Colloid and Interface Science*, *275*, 177–182.

Stepanov, A. L., Popok, V. N., Khaibullin, I. B., & Kreibig, U. (2002). Optical properties of polymethylmethacrilate with implanted silver nanoparticles. *Nuclear Instruments and Methods in Physics Research B*, *191*, 473–477.

Suflet, D. M., Chitanu, G. C., & Popa, V. I. (2006). Phosphorylation of polysaccharides: New results on synthesis and characterization of phosphorylated cellulose. *Reactive and Functional Polymer*, *66*, 1240–1249.

Tarimala, S., Kothari, N., Abidi, N., Hequet, E., Fralick, J., & Dai, L. L. (2006). New approach to antibacterial treatment of cotton fabric with silver nanoparticle-doped silica using sol–gel process. *Journal of Applied Polymer Science*, *101*, 2938–2943.

Thompson, D. S., Thompson, D. W., & Southward, R. E. (2002). Oxo-metal–polyimide nanocomposites. 2. Enhancement of thermal, mechanical, and chemical properties in soluble hexafluoroisopropylidine-based polyimides via the in situ formation of oxo-lanthanide (III)-polyimide nanocomposites. *Chemistry of Materials*, *14*, 30–37.

Wang, D., An, J., Luo, Q., Li, X., & Li, M. (2008). A convenient approach to synthesize stable silver nanoparticles and silver/polystyrene nanocomposite particles. *Journal of Applied Polymer Science*, *110*, 3038–3046.

Yong, W. K., Do Kyoung, L., Kyung, J. L., Byoung, R. M., Jong, H. K., Kim, Y. W., et al. (2007). In situ formation of silver nanoparticles within an amphiphilic graft copolymer film. *Journal of Polymer Science Part B: Polymer Physics*, *45*, 1283–1290.

Zeng, R., Rong, M. Z., Zhang, M. Q., Liang, H. C., Liang, H. C., & Zeng, H. M. (2002). Laser ablation of polymer-based silver nanocomposites. *Applied Surface Science*, *187*, 239–247.

Zhang, Z., & Han, M. (2003). One-step preparation of size-selected and well-dispersed silver nanocrystals in polyacrylonitrile by simultaneous reduction and polymerization. *Journal of Material Chemistry*, *13*, 641–643.

Zhao, C., Zhaob, Q., Zhao, Q., Qiu, J., Zhu, C., & Guo, S. (2007). Preparation and optical properties of Ag/PPy composite colloids. *Journal of Photochemistry and Photobiology A: Chemistry*, *187*, 146–151.

Zhu, C. Y., Xue, J. F., & He, J. H. (2009). Controlled in-situ synthesis of silver nanoparticles in natural cellulose fibers toward highly efficient antimicrobial materials. *Journal for Nanoscience and Nanotechnology*, *9*, 3067–3074.